Veterinary Medicine and Science

WILEY

ORIGINAL ARTICLE OPEN ACCESS

Dogs

Integrative Analysis of Dog Serum-Derived CircRNA Expression and Disease Severity, Inflammatory and Cardiac Damage Biomarkers Related to Canine Parvoviral Enteritis

Şükrü Değirmençay[1] | Selçuk Özdemir[2] | Sefa Küçükler[3] | Reyhane Bayat[1] | Muhammed Kadak[1]

[1]Department of Internal Medicine, Faculty of Veterinary Medicine, Atatürk University, Erzurum, Turkey | [2]Department of Genetic, Faculty of Veterinary Medicine, Atatürk University, Erzurum, Turkey | [3]Department of Biochemistry, Faculty of Veterinary Medicine, Atatürk University, Erzurum, Turkey

Correspondence: Şükrü Değirmençay (s.degirmencay@atauni.edu.tr)

Received: 13 March 2024 | **Revised:** 5 February 2025 | **Accepted:** 21 March 2025

Funding: This study was funded by the Scientific and Technological Research Council of Turkey (TUBITAK) (Grant 221O115) and the Research Fund of Atatürk University (Project TDA-2022-11265).

Keywords: canine parvovirus | circRNA | novel biomarker | RNA-seq

ABSTRACT

Background: The tissue- and developmental stage-specific expression of circular RNAs (circRNAs) makes them promising disease biomarkers. CircRNAs play a crucial role in regulating inflammatory responses; however, their function in canine parvovirus (CPV) infection remains largely unexplored.

Hypothesis: We hypothesized that circRNAs serve as biomarkers for disease severity, inflammation and organ damage in dogs with CPV.

Materials and Methods: The study included six dogs with mild CPV, six with severe CPV and six healthy controls. Haematological and biochemical parameters were analysed from blood samples. CircRNA profiling in serum samples was conducted through high-throughput sequencing, followed by bioinformatic analysis to identify potential circRNA biomarkers. Associations between circRNAs and haematological/biochemical markers were examined.

Results: The severe group exhibited significantly reduced leukocyte counts and elevated C-reactive protein (CRP) levels ($p < 0.05$). The mild group demonstrated higher levels of tumour necrosis factor-alpha (TNF-α), cardiac troponin I (cTnI) and creatine kinase myocardial band (CK-MB) ($p < 0.05$). Thus, the severe group experienced heightened inflammation, whereas the mild group demonstrated increased cardiac damage. Dogs with CPV expressed certain circRNAs differently (upregulated and downregulated), as revealed by gene ontology (GO) and Kyoto Encyclopaedia of Genes and Genomes (KEGG) enrichment analyses. Eighteen cicRNAs were identified as potential biomarkers. Bioinformatic and correlation analysis revealed that cfa_circ_6789, cfa_circ_6793, cfa_circ_6785, cfa_circ_6798, cfa_circ_6791, cfa_circ_6794 and cfa_circ_3119 could serve as biomarkers of inflammation and disease severity. Conversely, cfa_circ_3114, cfa_circ_3118, cfa_circ_3117, cfa_circ_3113, cfa_circ_3119, cfa_circ_1571, cfa_circ_6786 and cfa_circ_6794 were linked to cardiac damage.

Conclusions and Clinical Relevance: The identified circRNAs were actively involved in different stages of CPV infection and exhibited strong associations with disease onset and progression. They may play a key role in modulating infection pathogenesis while serving as potential biomarkers for inflammation and cardiac damage. This study is the first to investigate the role of circRNAs in CPV infection, providing novel insights into their diagnostic and prognostic potential.

1 | Introduction

Canine parvoviral enteritis (CPE) is one of the leading causes of morbidity and mortality in young dogs, particularly those aged 6 weeks to 6 months, worldwide (Mylonakis et al. 2016). Canine parvovirus (CPV), a single-stranded DNA virus belonging to the *Protoparvovirus* genus within the Parvoviridae family, is the causative agent of this disease (Mazzaferro 2020). It remains one of the most virulent and prevalent enteric diseases in dogs (Goddard and Leisewitz 2010). CPV-2 emerged following mutations approximately 10 years after the discovery of CPV-1 in the late 1960s. This strain is responsible for the widespread transmission of the disease in both adult and young dogs globally (Goddard and Leisewitz 2010).

In dogs, CPV primarily targets rapidly dividing cells in the gastrointestinal tract, bone marrow, lymphoid tissues and cardiac myocytes (Goddard and Leisewitz 2010). Infected animals develop leukopenia due to the destruction of leukocyte precursors in the bone marrow (Decaro and Buonavoglia 2012; Pollock 1982). The presence and severity of leukopenia during the disease course may serve as a prognostic indicator (Goddard et al. 2008).

Researchers have investigated biomarker changes associated with CPV infection in dogs. C-reactive protein (CRP) is among the most extensively studied parameters in this context. Acute inflammation or tissue damage triggers a rapid increase in CRP levels, which are typically low in the bloodstream (Kjelgaard-Hansen et al. 2003). CRP is widely utilized in both human and veterinary medicine for diagnosis, prognosis, treatment response monitoring and general health assessment (Eckersall and Bell 2010; Eckersall 2004). Elevated CRP concentrations have been identified as a reliable marker of disease severity and a predictor of mortality in CPV-infected dogs (Kocaturk et al. 2010).

In recent years, intensive research on the human genome has led to the identification of thousands of genes transcribing non-protein-coding RNAs (ncRNAs), which have emerged as potential biomarkers and therapeutic targets. The major categories of ncRNAs include microRNAs (miRNAs), long non-coding RNAs (lncRNAs) and circular RNAs (circRNAs) (Şentürk and Kömürcü Bayrak 2019). CircRNAs have garnered significant interest due to their high stability, abundance and conservation across mammalian cells (Conn et al. 2015). These molecules regulate gene expression through multiple mechanisms, including acting as miRNA sponges, interacting with RNA-binding proteins and modulating transcription. Notably, tissue-specific circRNA expression has been associated with the onset and progression of various diseases, including cancer, infections and cardiovascular and neurological disorders (Enuka et al. 2016; Zhong et al. 2018).

The growing interest in ncRNAs in human medicine has extended to veterinary research. However, studies examining ncRNAs in CPV infection remain scarce, with only a few reports focusing on miRNAs (Chuammitri et al. 2020; Zhou et al. 2017). For instance, miR-1247-3p and its target genes in biological pathways have been suggested as potential diagnostic biomarkers and therapeutic agents in feline kidney cells infected with CPV-2c (Chuammitri et al. 2020). To date, no studies have investigated circRNAs in CPE. Therefore, this study aimed to analyse circRNA expression profiles using RNA sequencing (RNA-seq) in healthy dogs and naturally CPV-infected dogs. Additionally, it sought to explore the potential of circRNAs as RNA-based biomarkers for assessing disease severity, inflammation and organ damage.

2 | Materials and Methods

2.1 | Animal Materials

This study was performed according to the approved ethical guidelines of Atatürk University (protocol no. 2021/146). A power analysis conducted using G-Power 3.1.9.7 determined that at least 5 dogs per group were required to achieve a 99% statistical power with a 0.05 error rate. The study's animal material included unvaccinated dogs, all of which were Kangal crossbreeds, with a median age of 2.5 months (range: 1.5–4 months) and a median weight of 5.25 kg (range: 3–15 kg). The study consisted of three groups: two patient groups (mild and severe) and a control group (healthy). In total, 18 dogs were included, with each group consisting of 6 dogs (3 males and 3 females).

The patient groups consisted of unvaccinated and untreated dogs that tested positive for CPV antigen and negative for canine coronavirus and *Giardia* antigen in faecal samples using rapid diagnostic test kits (Anigen Rapid CPV/CCV/Giardia Ag Test Kit). Furthermore, the absence of canine distemper virus (CDV) antigen in ocular and nasal swab samples was confirmed using a rapid diagnostic test kit (Anigen Rapid CDV Ag Test Kit). Additionally, the presence of intestinal parasites was ruled out via microscopic examination of native faecal smears.

The classification of CPV-infected dogs as mild or severe was based on a modified version of the scoring protocol developed by Panda et al. (2009) and Kocaturk et al. (2015) (see Table S1). In this scoring system, each clinical parameter (stool consistency, depression, dehydration and leukocyte count) was rated from 0 to 3, proportional to the severity of the finding. Dogs with a total clinical score of 1–4 were classified as mild, while those scoring 9–12 were classified as severe. The control group consisted of clinically healthy dogs with normal clinical and haematological parameters, negative rapid diagnostic test kit results and no abnormalities in faecal microscopy. During clinical examinations, rectal temperature, heart rate and respiratory rate were recorded for all dogs.

2.2 | Blood Sampling

Blood samples were collected from all dogs' vena cephalica antebrachii in the following volumes: 4 mL with anticoagulant (EDTA) and 8.5 mL without. In tubes without anticoagulant, blood samples were centrifuged at 1107 relative centrifugal force (RCF) for 10 min after 15 min at room temperature to obtain serum samples. Prior to biochemical analysis and RNA extraction, serum samples were kept at −80°C. Haematological analyses were conducted immediately.

2.3 | Haematological Analyses

A haematology analyser (Abacus Junior Vet5, Hungary) was used to measure white blood cell (WBC), lymphocyte (LYM), monocyte (MON), neutrophil (NEU), eosinophil (EOS), basophil (BAS), red

blood cell (RBC), haemoglobin (HGB), haematocrit (HCT) and platelet (PLT) levels.

2.4 | Cytokine, Acute-Phase Protein and Routine Biochemical Analyses

The concentrations of interleukin-6 (IL-6)[a], tumour necrosis factor-alpha (TNF-α)[b], interferon-gamma (IFN-γ)[c], CRP[d] and cardiac troponin I (cTnI)[e] in serum samples were determined using dog-specific ELISA kits (SunRed Biotechnology Company, Shanghai, China, [a]CAT No: 201-15-0128, [b]Cat No: 201-15-0019 and [c]Cat No: 201-15-0173, BT Lab Bioassay Technology Laboratory sandwich kit, Shanghai, China, [d]CAT No: E0124Ca and [e]CAT No: E0069Ca). The sensitivity and assay range for IL-6 were 0.047 and 0.05–15 pg/mL, respectively. These values for TNF-α were 0.028 and 0.03–9 pg/mL; IFN-γ were 5.448 and 6–180 ng/L; CRP were 0.028 and 0.05–30 mg/L; and cTnI were 2.61 and 5–1500 ng/L. Serum albumin (ALB), alanine aminotransferase (ALT), blood urea nitrogen (BUN), creatinine (CREA) and creatine kinase myocardial band (CK-MB) levels were measured using an autoanalyser (Mindray BS-240, Guangdong, China).

2.5 | Detection of CPV and CircRNAs

2.5.1 | Detection of CPV by Real-Time PCR (RT-PCR)

Unlike conventional PCR, which detects DNA, RT-PCR amplifies viral RNA, allowing for the sensitive detection of actively replicating CPV particles in infected tissues (Segev et al. 2022). CPV detection was performed using primers designed with Primer-3 design software. The sequences of the forward and reverse primers were as follows: 5′-TTGAGGCGTCTACACAAGGA-3′ and 5′-GGTGTTTCTCCTGTTGTGGT-3 which target highly conserved regions of the CPV VP2 gene. Each RT-PCR reaction was carried out in a final volume of 25 μL containing 11 μL of deionized sterile water, 12.5 μL of Syber Green Master Mix (Qiagen, Germany), 1 pmol of each primer and 2 μL of DNA template. Thermal cycling conditions for amplification included 1 cycle of 4 min at 94°C, 40 cycles of 30 s at 94°C, 45 s at 59°C and 45 s at 72°C; the final extension step was performed at 72°C for 5 min. Positive and negative controls were included in each analysis.

2.6 | Detection of CircRNAs

2.6.1 | RNA Extraction and Quality Control for Sequencing

Total RNA was isolated from 200 μL serum samples with the miRNeasy Serum/Serum Kit (Qiagen, Hilden, Germany) following the manufacturer's instructions. Total RNA concentration was measured by a NanoDrop spectrophotometer (Epoch microplate spectrophotometer) at 260 nm. RNA integrity number (RIN) was determined with an Agilent Bioanalyzer. Total RNA with >7.5 RIN was used for sequencing.

2.6.2 | High-Throughput Sequencing

For the sequencing, 12 samples from CPV-positive dogs and 6 samples from healthy dogs were used. RNA-seq was carried out by Novogene UK Company Limited, United Kingdom. Briefly, the Ribo-Zero rRNA Removal Kit (Illumina, San Diego, CA, USA) and the CircRNA Enrichment Kit (Cloud-Seq, USA) were used to eliminate the rRNA and get more circRNAs. RNA libraries were prepared with the TruSeq Stranded Total RNA Library Prep Kit (Illumina, San Diego, CA, USA), and the quality and quantity of the libraries were analysed with the BioAnalyzer 2100 system (Agilent Technologies Inc., Santa Clara, CA, USA). After complementary DNA (cDNA) was produced, the cDNA products were sequenced with the Illumina HiSeq 4000 sequencer (Illumina, San Diego, CA, USA) following the manufacturer's instructions.

2.6.3 | Bioinformatic Analysis of CircRNAs

All reads were acquired from the Illumina HiSeq 4000 sequencer, and the quality control of reads was addressed by Q20 and Q30. The 3′ adaptor was trimmed with Cutadapt software (v1.9.3), and the poor-quality reads were removed with Cutadapt software (v1.9.3). The high-quality reads were aligned to the reference genome/transcriptome using STAR software, and CIRCexplorer2 software was used to identify circRNAs. The identified circRNAs were annotated with both the Circ2Trait database and the circBase database. The differentially expressed circRNAs were detected with edgeR software (DESeq2 R package). The functions of differentially expressed circRNAs were predicted by using gene ontology (GO) and Kyoto Encyclopaedia of Genes and Genomes (KEGG) analysis (KOBAS software).

2.6.4 | RT-PCR for CircRNA Expression

Total RNA was isolated from 200 μL serum samples using the miRNeasy Serum/Serum Kit (Qiagen, Hilden, Germany) in accordance with the manufacturer's instructions. The concentration of total RNA was quantified using a NanoDrop spectrophotometer (Epoch microplate spectrophotometer) at a wavelength of 260 nm. Subsequently, cDNA was synthesized with the QuantiTect Reverse Transcription Kit (Qiagen, Germany) as per the manufacturer's instructions. Each primer was prepared at a final concentration of 0.2 μM. The relative expression of circRNA was quantified using the Rotor-Gene Q MDx 5plex HRM system (CA), with β-actin employed as an internal control (Özdemir et al. 2022). The relative expression levels were calculated using the $2^{-\Delta\Delta Ct}$ method (Livak and Schmittgen 2001).

2.7 | Statistical Analysis

Statistical analysis was conducted using SPSS 25.0 (SPSS Inc., Chicago, IL, USA). Normality was evaluated through the Shapiro–Wilk test. Comparative analysis of parameters between groups was performed using one-way analysis of variance (ANOVA), followed by post hoc Duncan tests. For correlation analysis, Pearson's method was applied for parametric data, whereas Spearman's method was employed for nonparametric data. Correlation coefficients were interpreted as follows: weak (0.10–0.39), moderate (0.40–0.69), strong (0.70–0.89) and very strong (0.90–1.00) (Mukaka 2012; Overholser 2008). To determine the best predictive parameter for disease severity and cardiac damage among the groups, receiver operating characteristic

TABLE 1 | Comparison of haematological, biochemical and some clinical parameters of dogs in the patient and control groups.

Parameters	Control group (*n*:6)	Mild group (*n*:6)	Severe group (*n*:6)	*p*
WBC (x10^3/μL)	9.57 ± 2.94^B	10.18 ± 1.93^B	1.64 ± 1.03^A	0.000
LYM (x10^3/μL)	1.78 ± 0.75^B	2.04 ± 1.26^B	0.70 ± 0.33^A	0.041
MON (x10^3/μL)	0.61 ± 0.25^B	0.54 ± 0.33^B	0.08 ± 0.05^A	0.003
NEU (x10^3/μL)	6.88 ± 2.41^B	7.56 ± 1.84^B	0.8 ± 0.75^A	0.000
EOS (x10^3/μL)	0.25 ± 0.33	0.018 ± 0.007	0.045 ± 0.028	0.106
BAS (x10^3/μL)	0.058 ± 0.081	0.018 ± 0.009	0.018 ± 0.012	0.277
RBC (x10^6/μL)	5.93 ± 0.57	6.19 ± 0.54	6.77 ± 0.57	0.053
HGB (g/dL)	11.93 ± 1.75	11.38 ± 1.81	13.45 ± 1.05	0.094
HCT (%)	37.09 ± 4.25	41.49 ± 4.90	43.03 ± 5.37	0.124
PLT (x10^3/μL)	304.33 ± 127.20	497.83 ± 232.74	536.33 ± 155.50	0.083
IL-6 (pg/mL)	0.8072 ± 0.10224^A	1.2322 ± 0.33029^B	1.1160 ± 0.14211^B	0.011
TNF-α (pg/mL)	0.4038 ± 0.03825^A	0.5817 ± 0.06778^B	0.4633 ± 0.13488^A	0.012
IFN-γ (ng/L)	112.39 ± 6.41	149.84 ± 42.65	139.17 ± 48.21	0.234
CRP (mg/L)	0.448 ± 0.029^A	1.005 ± 0.666^{AB}	1.907 ± 1.143^B	0.015
ALB (g/dL)	2.52 ± 0.08^B	2.16 ± 0.15^A	2.20 ± 0.16^A	0.001
cTnI (ng/L)	45.67 ± 8.14^A	148.17 ± 24.69^C	89.17 ± 36.26^B	0.000
CK-MB (U/L)	508.85 ± 156.82^A	1135.17 ± 279.53^B	776.90 ± 353.74^A	0.005
ALT (U/L)	22.83 ± 16.27	46.33 ± 50.96	18.50 ± 8.24	0.282
BUN (mg/dL)	10.05 ± 2.23^A	16.98 ± 13.72^{AB}	26.93 ± 11.59^B	0.042
CREA (mg/dL)	0.32 ± 0.15^{AB}	0.18 ± 0.77^A	0.49 ± 0.25^B	0.026
HR (beats/min)	78.33 ± 4.63^A	119.67 ± 19.45^B	129 ± 29.76^B	0.002
RR (breaths/min)	28.33 ± 4.28	38.67 ± 7.45	34.83 ± 14.35	0.206
RT (°C)	37.43 ± 0.23^A	38.43 ± 0.39^B	39.30 ± 1.14^B	0.001

Note: Data are presented as mean ± standard deviation. Different letters in the superscript are statistically significant ($p < 0.05$).

Abbreviations: ALB, albumin; ALT, alanine aminotransferase; BAS, basophil; BUN, blood urea nitrogen; CK-MB, creatine kinase myocardial band; CREA, creatinine; CRP, C-reactive protein; cTnI, cardiac troponin-I; EOS, eosinophil; HCT, haematocrit; HGB, haemoglobin; HR, heart rate/min; IFN-γ, interferon gamma; IL-6, interleukin-6; LYM, lymphocyte; MON, monocytes; NEU, neutrophil; PLT, platelet; RBC, red blood cell; RR, Respiratory frequency/min; RT, rectal temperature;TNF-α, tumour necrosis factor-alpha; WBC, white blood cell.

(ROC) curve analysis was conducted using MedCalc version 20 (Mariakerke, Belgium). Sensitivity, specificity and the area under the curve (AUC) were calculated for each variable. The AUC values were classified as follows: bad (0.50–0.60), poor (0.60–0.70), fair (0.70–0.80), good (0.80–0.90) and excellent (0.9–1) (Swets 1988). Scatter diagrams were generated using GraphPad Prism 8 (San Diego, CA, USA). Spearman's correlation test was specifically applied to analyse the relationship between marker candidate circRNAs and biochemical parameters. All statistical tests were conducted at a significance level of $p < 0.05$.

3 | Results

3.1 | Clinical Findings

Compared to the control group, both the mild and severe groups had higher heart rates ($p = 0.002$) and rectal temperatures ($p = 0.001$). The severe group exhibited the highest heart rate and rectal temperature (Table 1). The median age of the mild, severe, and the control gropus was 2.25 months (range: 2-3 months), 2.75 months (range: 1.5-4 months), and 2.25 months (range:1.5-3 months), respectively. Similarly, the median body wieght was 5.25 kg (range: 5-6.30 kg) in the mild group, 5.75 kg (range: 4-15 kg) in the severe group, and 4.75 kg (range: 3-6.40 kg) in the control group. Clinically, anorexia, vomiting, weakness and mild dehydration were common in the mild group, whereas anorexia, weakness, vomiting, diarrhoea and moderate dehydration were more prevalent in the severe group.

3.2 | Haematological Findings

No significant difference in leukocyte counts was observed between the mild and control groups, whereas the severe group exhibited marked leukopenia ($p < 0.001$), along with statistically significant lymphopenia ($p = 0.041$), monocytopenia ($p = 0.003$) and neutropenia ($p < 0.001$). Both the mild and severe groups showed non-significant increases in RBC, HCT and PLT levels (Table 1).

TABLE 2 | Area under the curve (AUC), optimum cut-off values (cut-off), sensitivity, specificity, standard error (SEM) and significance values (p) of the selected parameters in detecting disease severity and heart damage between mild and control groups.

Parameters	IL-6 (pg/mL)	TNF-α (pg/mL)	IFN-γ (ng/L)	CRP (mg/L)	ALB (g/dL)	WBC (x10^3/μL)	HCT (%)	PLT (x10^3/μL)	cTnI (ng/L)	CK-MB (U/L)
AUC	0.903	1.000	0.917	1.000	0.986	0.556	0.819	0.792	1.000	1.000
Cut-off	>0.98	>0.45	>123.39	>0.478	≤2.3	>8.3	>39.7	>342	>60	>760
Sensitivity (%)	83.3	100	83.3	100	83.3	83.3	83.3	83.3	100	100
Specificity (%)	100	100	100	100	100	50	83.3	83.3	100	100
SEM	0.103	0.000	0.0913	0.000	0.0196	0.194	0.137	0.148	0.000	0.000
p value	<0.001	<0.001	<0.001	<0.001	<0.001	0.775	0.020	0.049	<0.001	<0.001

Abbreviations: ALB, albumin; CK-MB, creatine kinase myocardial band; CRP, C-reactive protein; cTnI, cardiac troponin-I; HCT, haematocrit; IFN-γ, interferon gamma; IL-6, interleukin-6; PLT, platelet; TNF-α, tumour necrosis factor-alpha; WBC, white blood cell.

3.3 | Cytokine, Acute-Phase Protein and Routine Biochemical Analysis Findings

IL-6, TNF-α, cTnI and CK-MB levels were higher in the mild group compared to the control group ($p < 0.05$), whereas IL-6, CRP, cTnI and BUN levels were higher in the severe group ($p < 0.05$). Both patient groups had lower ALB levels than the control group ($p = 0.001$) (Table 1).

In the correlation analysis, CRP was moderately negatively correlated with WBC ($r = -0.508$, $p = 0.032$), MON ($r = -0.515$, $p = 0.029$), NEU ($r = -0.476$, $p = 0.046$), HCT ($r = 0.698$, $p = 0.001$) and PLT ($r = 0.607$, $p = 0.008$). IL-6 was moderately negatively correlated with ALB ($r = -0.601$, $p = 0.008$), whereas it was moderately positively correlated with cTnI ($r = 0.594$, $p = 0.009$) and CK-MB ($r = 0.483$, $p = 0.042$). TNF-α had a moderate positive correlation with cTnI ($r = 0.559$, $p = 0.016$), whereas ALB had a moderate negative correlation with cTnI ($r = -0.599$, $p = 0.009$). A very strong positive correlation was found between cTnI and CK-MB ($r = 0.941$, $p = 0.000$). Rectal temperature (RT) had a moderate negative correlation with WBC ($r = -0.608$, $p = 0.007$), NEU ($r = -0.572$, $p = 0.013$), MON ($r = -0.500$, $p = 0.035$) and ALB ($r = -0.577$, $p = 0.012$).

ROC analysis results for mild and control groups are shown in Table 2 and Figures S1 and S2. CRP, TNF-α, ALB, IFN-γ and IL-6 were found to be excellent indicators of inflammation, respectively. To detect inflammation, CRP levels above 0.478 mg/L and TNF-α above 0.45 pg/mL showed 100% sensitivity and specificity. cTnI > 60 ng/L and CK-MB > 760 U/L were determined as excellent markers in detecting cardiac damage with 100% sensitivity and 100% specificity.

ROC analysis results for severe and control groups are shown in Table 3 and Figures S3 and S4. CRP, ALB and IL-6 were found to be excellent indicators of inflammation, respectively. CRP > 0.478 mg/L detected inflammation with 100% sensitivity and specificity. cTnI was determined as an excellent marker, better detecting cardiac damage with 100% sensitivity and 83.3% specificity above 50 ng/L.

Table S2 and Figures S5 and S6 display the findings of the ROC analysis between the mild and severe groups. WBC and CRP were found to be excellent and good markers, respectively, for evaluating disease severity. WBC values ≤2.84×10^3/μL accurately predicted disease severity with 100% sensitivity and specificity. CRP values above 0.811 mg/L predicted disease severity with 100% sensitivity and 66.7% specificity. CTnI ≤ 109 ng/L and CK-MB ≤ 813.2 U/L predicted cardiac damage with 83.3% sensitivity and 100% specificity and were determined as excellent and good markers, respectively.

3.4 | RT-PCR Results for CPV Detection

The control group had negative RT-PCR results for CPV, whereas the patient groups had positive results (see Table S3).

3.5 | Quality Control Results

The RNA-seq results were subjected to quality control analysis. For RNA-seq, Q20, Q30 and QC rates were found to be ideal. Additionally, the overall G data achieved the desired level (Table S4). These results showed that the RNA-seq results were accurate and reliable. The Python 3.9 programme's analyses based on error rate and guanine/cytosine (GC) content confirmed that the results were at the desired level (Figure 1x and y).

3.6 | Detected CircRNA Lengths

The lengths of the circRNAs identified and characterized by sequencing ranged between 100 and 700 nt (Figure 1z). Additionally, Figure 2 displays the circos distributions of circRNAs.

3.7 | Mapping and RNA Distributions

It was determined that the majority of the characterized circRNAs were expressed on the X chromosome and the first chromosome, regulating genes on these chromosomes (Figure 3). The classification of mapped reads for each group is as follows:

For the control group: The protein-coding RNA ratio was 20.2%, mitochondrial mRNA ratio was 0.8%, miRNA ratio was 0.3%, mitochondrial tRNA ratio was 0%, pseudogene ratio was 0%, misc RNA ratio was 0%, and retrotransposon rate was 0%.

TABLE 3 | Area under the curve (AUC), optimum cut-off values (cut-off), sensitivity, specificity, standard error (SEM) and significance values (p) of the selected parameters in detecting disease severity and heart damage between severe and control groups.

Parameters	IL-6 (pg/mL)	TNF-α (pg/mL)	IFN-γ (ng/L)	CRP (mg/L)	ALB (g/dL)	WBC (x10^3/μL)	HCT (%)	PLT (x10^3/μL)	cTnI (ng/L)	CK-MB (U/L)
Area	0.972	0.569	0.667	1.000	0.986	0.556	0.806	0.917	0.972	0.778
Cut-off	>0.87	>0.45	>123.39	>0.478	≤2.3	≤2.84	>38.6	>342	>50	>582.3
Sensitivity (%)	100	50	50	100	83.3	83.3	83.3	100	100	66.7
Specificity (%)	83.3	100	100	100	100	50	66.7	83.3	83.3	83.3
SEM	0.0393	0.205	0.183	0.000	0.0196	0.194	0.135	0.0913	0.0393	0.145
p value	<0.001	0.735	0.361	<0.001	<0.001	0.775	0.024	<0.001	<0.001	0.055

Abbreviations: ALB, albumin; CK-MB, creatine kinase myocardial band; CRP, C-reactive protein; cTnI, cardiac troponin-I; HCT, haematocrit; IFN-γ, interferon gamma; IL-6, interleukin-6; PLT, platelet; TNF-α, tumour necrosis factor-alpha; WBC, white blood cell.

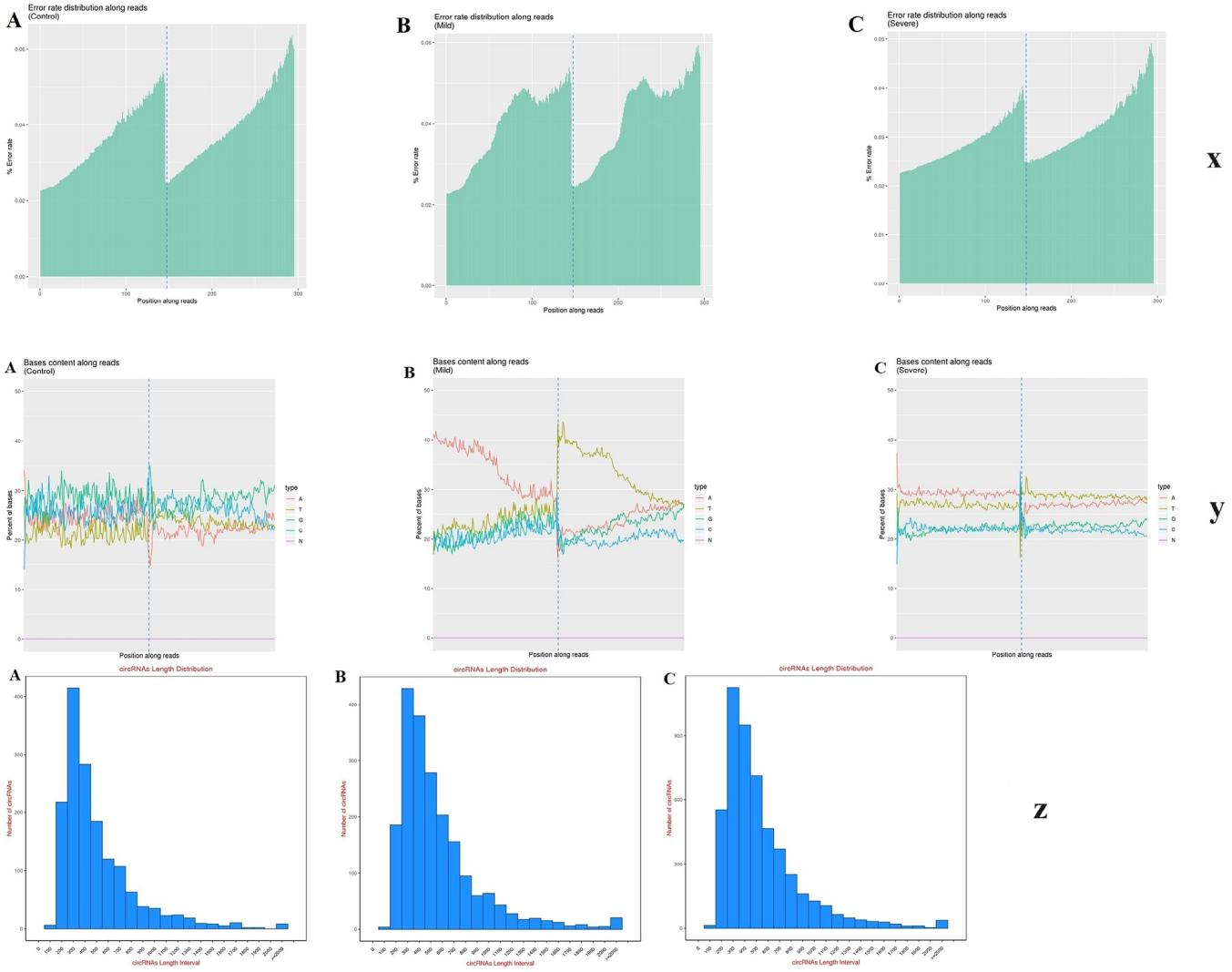

FIGURE 1 | It shows the quality control parameters of RNA sequencing. (x) It represents the false rate percentages of sequencing (error_rate [%]). (A) Control, (B) mild and (C) severe, (y) it represents the guanine/cytosine content (GC_content [%]). (A) Control, (B) mild and (C) severe, (z) it represents the lengths (nt) of the characterized circRNAs. (A) Control, (B) mild and (C) severe. circRNAs, circular RNAs.

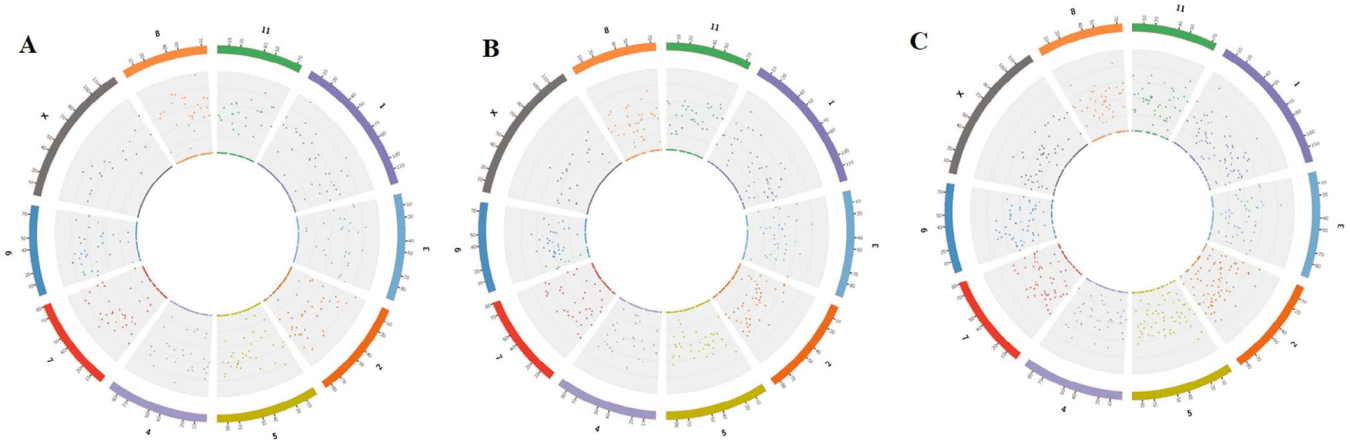

FIGURE 2 | It shows on which chromosome the characterized circRNAs are localized. The circos results of the characterized circRNAs (on the chromosome). (A) Control, (B) mild and (C) severe.

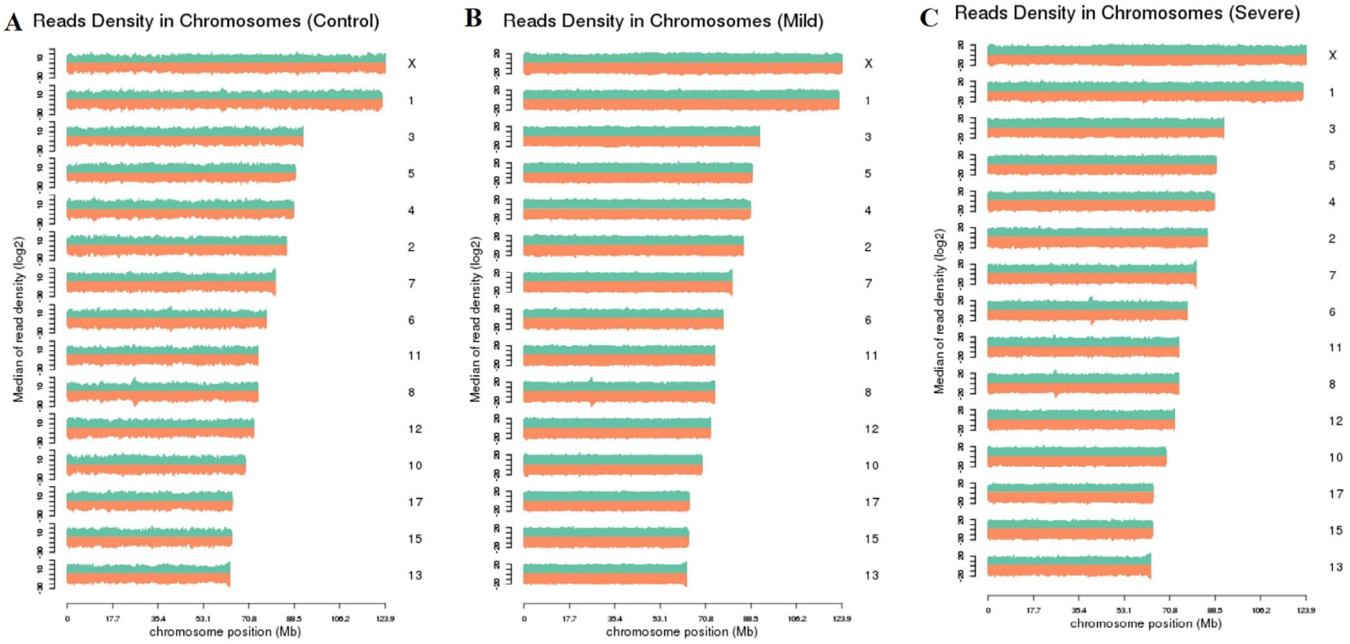

FIGURE 3 | It shows the read densities of the characterized circRNAs on the chromosome. (A) Control, (B) mild and (C) severe.

For the mild group: The protein-coding RNA ratio was 12.7%; mitochondrial mRNA ratio was 1.3%, miRNA ratio was 0.1%, mitochondrial tRNA ratio was 0%, pseudogene ratio was 0%, misc RNA ratio was 0%, and retrotransposon rate was 0%.

For the severe group: The protein-coding RNA ratio was 10.3%, mitochondrial mRNA ratio was 1%, miRNA ratio was 0.1%, mitochondrial tRNA ratio was 0%, pseudogene ratio was 0%, misc RNA ratio was 0%, and retrotransposon ratio was 0% (Figure 4x).

3.8 | Differentially Expressed CircRNAs

CircRNAs were considered differentially expressed on the basis of the RNA-seq results when their expression changed by at least twofold with a p value < 0.05. A total of 541 circRNAs were upregulated and 868 circRNAs were downregulated when the mild group was compared to the control group. In the severe versus control group comparison, 25 circRNAs were upregulated and 1081 circRNAs were downregulated. When comparing the mild and severe groups, 753 circRNAs were upregulated, whereas 21 circRNAs were downregulated (Figure 4y).

CircRNAs were selected on the basis of their log2-fold changes among the control, mild and severe groups, and 18 candidate biomarker circRNAs were identified. These circRNAs are listed in Table 4. Figure 5 also displays a heatmap showing the circRNA-based expression differences between the groups.

When Table 4 was examined, it was found that cfa_circ_1570, cfa_circ_1574 and cfa_circ_1575 were expressed in the control group. cfa_circ_3114, cfa_circ_3117, cfa_circ_3118 and cfa_circ_3119 were only expressed in the mild group, whereas cfa_circ_6784, cfa_circ_6785, cfa_circ_6786, cfa_circ_6789,

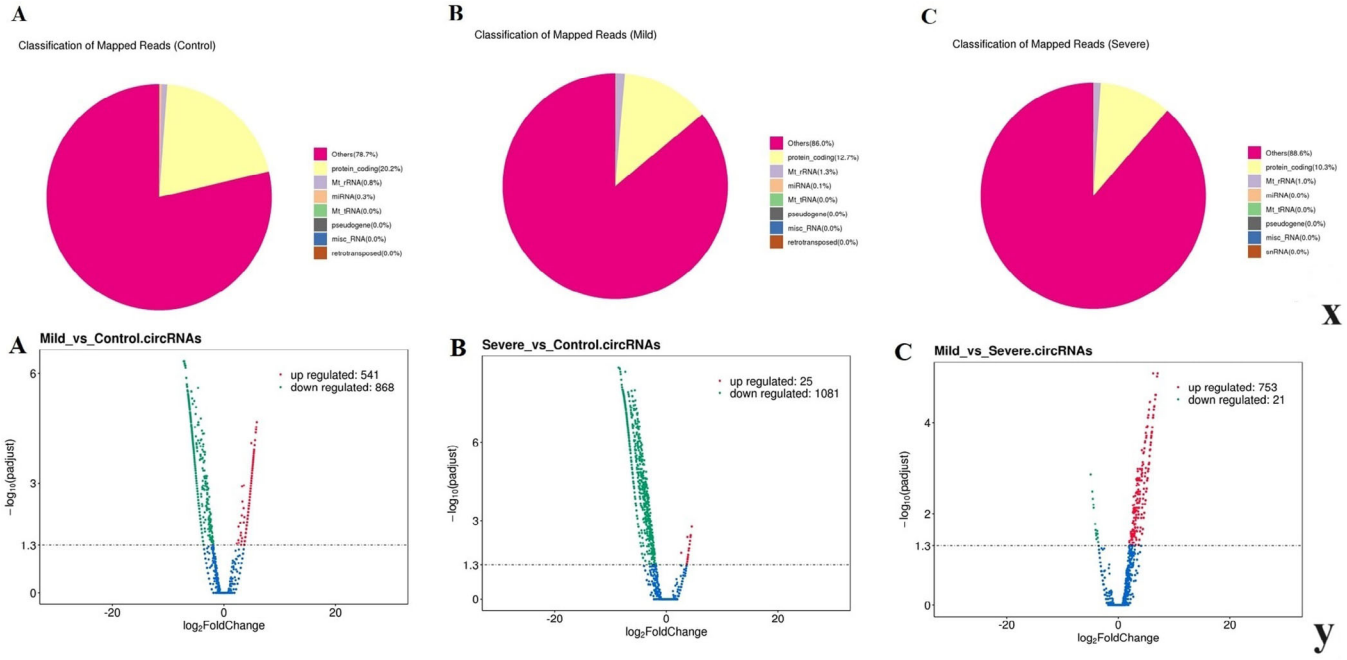

FIGURE 4 | It shows subtyping of data obtained from sequencing. (x) Classification of the obtained readings. (A) Control, (B) mild and (C) severe, (y) circRNAs differentially expressed between groups. (A) Mild to control, (B) severe to control and (C) mild to severe. circRNAs, circular RNAs.

TABLE 4 | circRNA-based biomarker candidates.[a]

ID		Control	Mild	Severe
cfa_circ_1570	0.930889219647253	0	0	
cfa_circ_1574	0.39612307219032	0	0	
cfa_circ_1575	0.574378454675964	0	0	
cfa_circ_1571	0.039612307219032	0.0251166385297524	0.0898509543384339	
cfa_circ_3113	0	0.301399662357028	0.329453499240924	
cfa_circ_3114	0	0.175816469708266	0	
cfa_circ_3117	0	0.301399662357028	0	
cfa_circ_3118	0	0.351632939416533	0	
cfa_circ_3119	0	0.200933108238019	0	
cfa_circ_6784	0	0	0.23960254490249	
cfa_circ_6785	0	0	0.209652226789679	
cfa_circ_6786	0	0	0.0898509543384339	
cfa_circ_6789	0	0	0.179701908676868	
cfa_circ_6791	0	0	0.628956680369037	
cfa_circ_6793	0	0	0.0898509543384339	
cfa_circ_6794	0	0	0.149751590564056	
cfa_circ_6795	0	0	0.149751590564056	
cfa_circ_6798	0	0	0.119801272451245	

[a]This table shows the differential expression of circRNAs by groups.

cfa_circ_6791, cfa_circ_6793, cfa_circ_6794, cfa_circ_6795 and cfa_circ_6798 were detected only in the severe group. cfa_circ_1571 was found to be expressed in all groups. cfa_circ_3113 was expressed in both mild and severe groups.

Table 5 displays the correlation analysis between candidate biomarker circRNAs and biochemical parameters. TNF-α and cfa_circ_1570 showed a strong positive correlation ($r = 0.802$, $p = 0.002$).

TABLE 5 | Correlation results of candidate circular RNAs (circRNAs) and biochemical parameters among patient groups (Spearman).

	Circ 1570	Circ 1571	Circ 3113	Circ 3114	Circ 3117	Circ 3118	Circ 3119	Circ 6784	Circ 6785	Circ 6786	Circ 6789	Circ 6791	Circ 6793	Circ 6794	Circ 6795	Circ 6798
IL-6	0.112	−0.240	0.296	0.082	0.030	0.082	0.131	−0.119	−0.007	−0.127	−0.164	0.045	−0.007	−0.142	0.067	0.07
TNF-α	0.802**	−0.396	−0.039	0.411	0.490	0.411	0.374	−0.203	−0.411	−0.157	−0.455	−0.321	−0.321	−0.470	−0.328	−0.314
IFN-γ	0.144	−0.406	0.060	0.105	0.064	0.105	0.430	−0.336	−0.060	−0.306	−0.090	−0.187	−0.172	−0.082	−0.239	−0.149
CRP	−0.455	0.353	−0.169	−0.564	−0.542	−0.564	−0.591*	0.503	0.658*	0.496	0.735**	0.593*	0.668*	0.579*	0.504	0.623*
ALB	0.039	0.352	−0.072	−0.211	−0.076	−0.211	−0.171	0.312	0.249	0.094	0.278	0.219	0.301	0.027	0.137	0.251
cTnI	0.378	−0.742**	0.716**	0.836**	0.804**	0.836**	0.613*	−0.378	−0.512	−0.679*	−0.567	−0.493	−0.493	−0.612*	−0.537	−0.485
CK-MB	0.322	−0.608*	0.748**	0.717**	0.729**	0.717**	0.482	−0.266	−0.370	−0.627*	−0.448	−0.381	−0.381	−0.500	−0.433	−0.366

Abbreviations: ALB, albumin; CK-MB, creatine kinase myocardial band; CRP, C-reactive protein; cTnI, cardiac troponin-I; IFN-γ, interferon gamma; IL-6, interleukin-6; TNF-α, tumour necrosis factor-alpha.

*$p < 0.05$.

**$p < 0.01$.

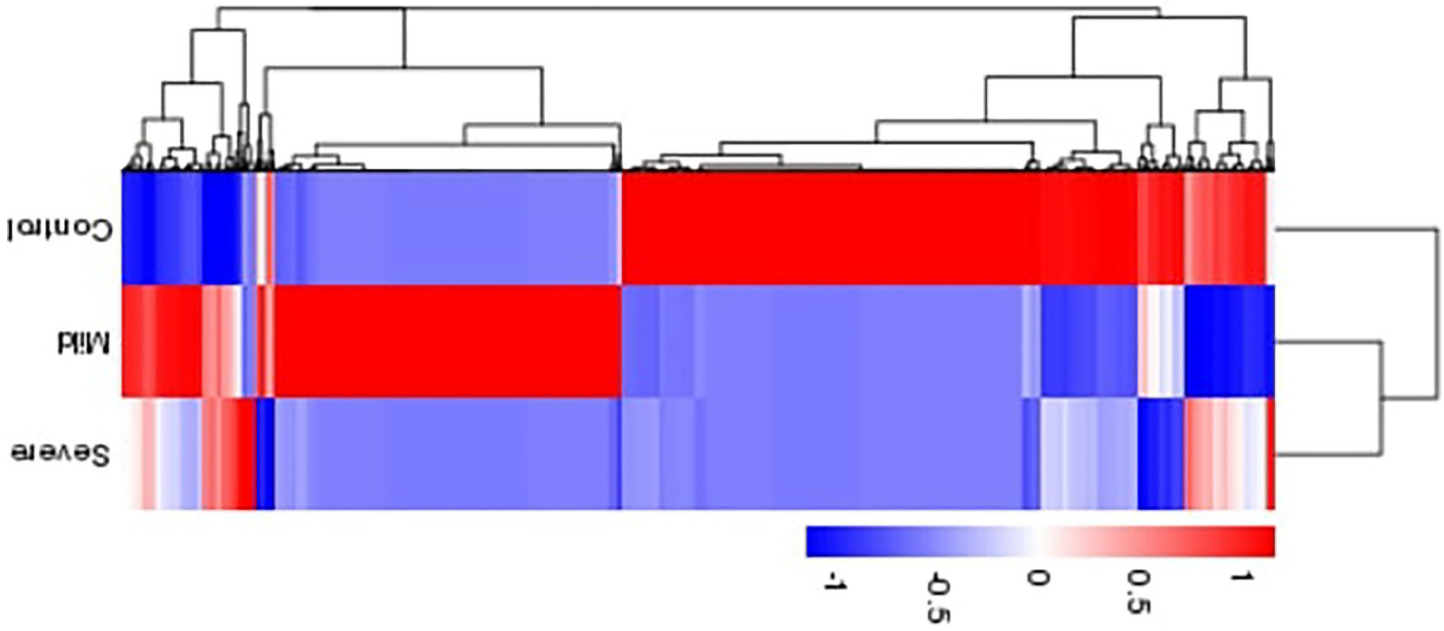

FIGURE 5 | Heatmap cluster visualization displays the variation in expression of circular RNAs categorized by groups. The colours red, blue and white represent upregulated, downregulated and no difference, respectively.

A strong positive correlation was observed between CRP and cfa_circ_6789 ($r = 0.735$, $p = 0.006$). cfa_circ_6793 ($r = 0.668$, $p = 0.018$), cfa_circ_6785 ($r = 0.658$, $p = 0.02$), cfa_circ_6798 ($r = 0.623$, $p = 0.03$), cfa_circ_6791 ($r = 0.593$, $p = 0.042$) and cfa_circ_6794 ($r = 0.579$, $p = 0.049$) showed moderate positive correlations with CRP. cfa_circ_3119 showed a moderate negative correlation with CRP ($r = -0.591$, $p = 0.043$).

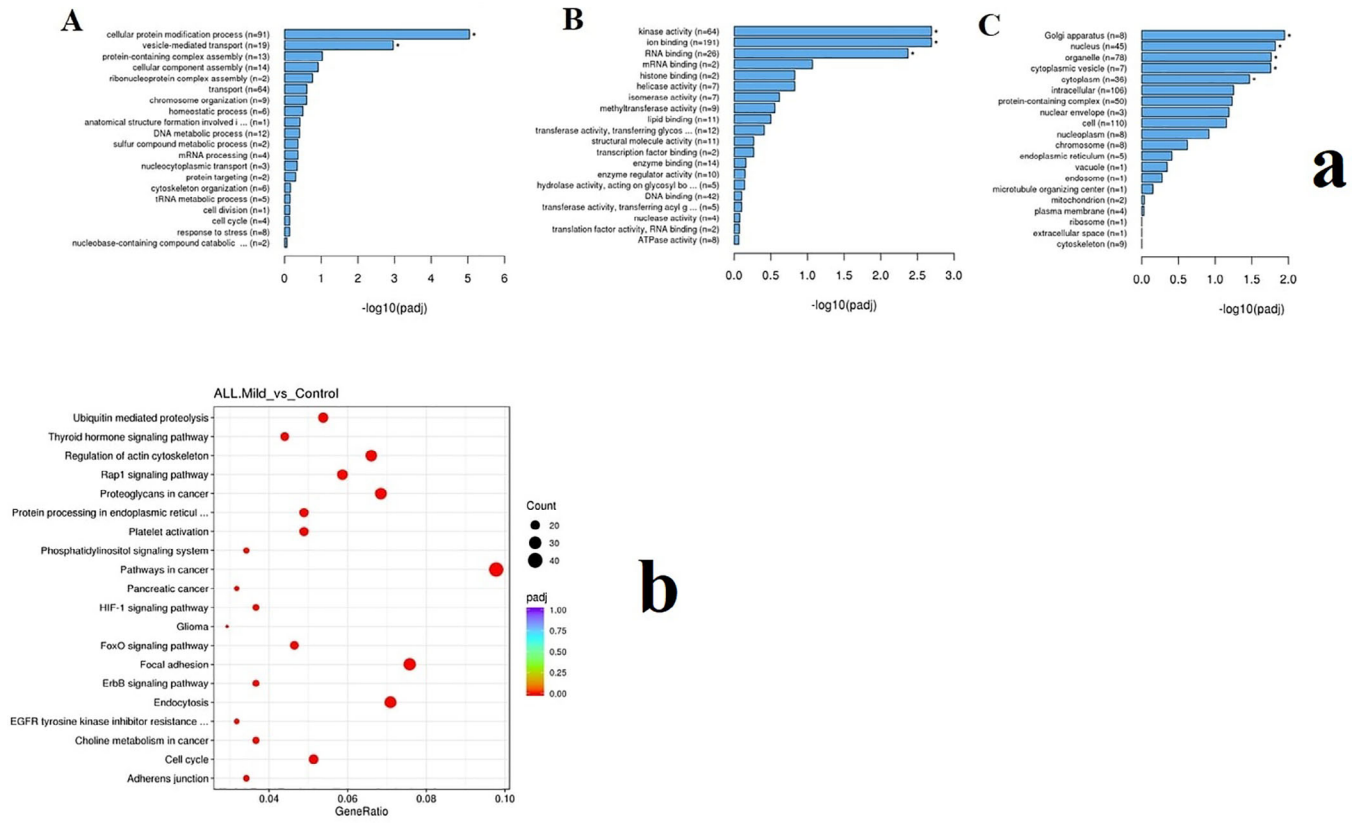

FIGURE 6 | (a) Gene ontology (GO) analysis of differentially expressed circRNAs. (A) It shows the biological process, (B) it shows the metabolic process and (C) it shows the cellular localization (b) KEGG pathway analysis of detected circRNAs.

A strong positive correlation was found between cTnI and cfa_circ_3114 ($r = 0.836$, $p = 0.001$), cfa_circ_3118 ($r = 0.836$, $p = 0.001$), cfa_circ_3117 ($r = 0.804$, $p = 0.002$) and cfa_circ_3113 ($r = 0.716$, $p = 0.009$). cTnI moderately positively correlated with cfa_circ_3119 ($r = 0.613$, $p = 0.034$). A strong negative correlation was observed between cTnI and cfa_circ_1571 ($r = -0.742$, $p = 0.006$), whereas cfa_circ_6786 ($r = -0.679$, $p = 0.015$) and cfa_circ_6794 ($r = -0.612$, $p = 0.034$) showed moderate negative correlations with cTnI.

A strong positive correlation was found between CK-MB and cfa_circ_3113 ($r = 0.748$, $p = 0.005$), cfa_circ_3117 ($r = 0.729$, $p = 0.007$), cfa_circ_3114 ($r = 0.717$, $p = 0.009$) and cfa_circ_3118 ($r = 0.717$, $p = 0.009$). Moderate negative correlations were found between CK-MB and cfa_circ_6786 ($r = -0.627$, $p = 0.029$) and cfa_circ_1571 ($r = -0.608$, $p = 0.036$).

3.9 | GO and KEGG Pathway Analysis of Differentially Expressed CircRNAs

The detected circRNAs were primarily involved in molecular functions such as kinase activity, iron binding and RNA binding. They were also associated with biological processes, including cellular protein modification (e.g., post-translational modifications) and vesicle-mediated transport, both of which are crucial for immune signalling and viral replication in CPV. The Golgi apparatus, nucleus, organelles and cytoplasm were the main cellular locations where these circRNAs were active (Figure 6a).

KEGG pathway analysis revealed that most of the detected circRNAs were linked to cancer-related pathways. Additionally, circRNAs were involved in focal adhesion, endocytosis and ErbB signalling pathways. Finally, they participated in Rab1 signalling, ubiquitin-mediated proteolysis and thyroid hormone signalling (Figure 6b).

3.10 | Confirmation of CircRNAs by RT-PCR

RT-PCR confirmed that the RNA-seq results provided the same expression profiles (Figure 7).

4 | Discussion

In this study, we examined the expression profiles of circRNAs in dogs infected with CPV. Additionally, we identified candidate circRNAs that could serve as biomarkers for disease severity, inflammation and organ damage.

Leukocyte parameters and ALB levels were significantly lower, whereas CRP levels were significantly higher in the severe group ($p < 0.05$). CPV infection induces leukopenia and neutropenia, which exacerbate disease severity and mortality rates (Goddard et al. 2008; Kalli et al. 2010; Mason et al. 1988; Brunner 1985). CRP levels have been shown to predict prognosis, disease severity and mortality in CPV-infected dogs (Kocaturk et al. 2010; Kocaturk et al. 2015). Our study found that CRP levels in the severe group

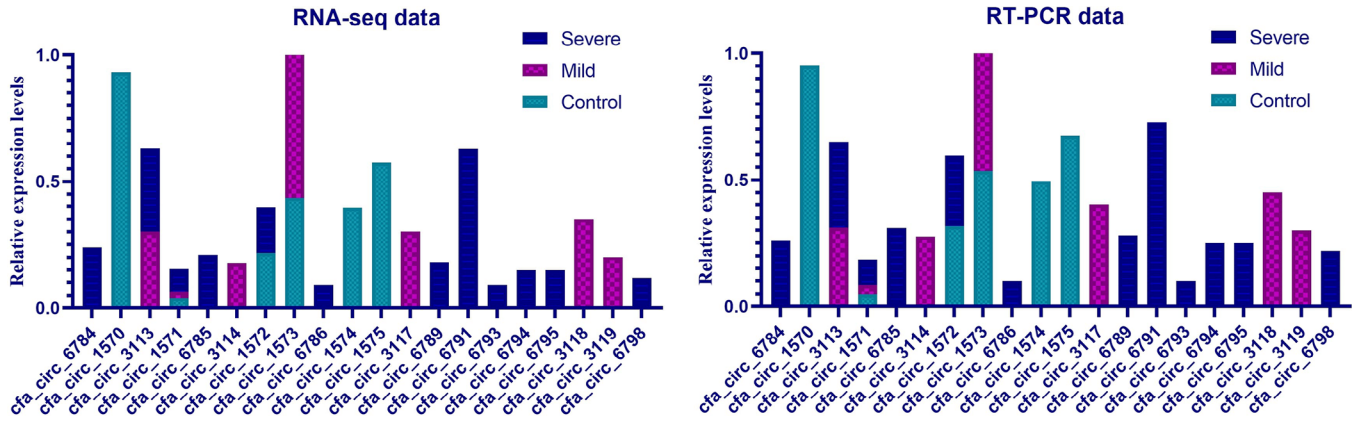

FIGURE 7 | Comparison of RNA sequencing and RT-PCR results. RT-PCR, real-time PCR; RNA-seq, RNA sequencing.

were four times higher than in the control group. CRP levels exceeding 0.811 mg/L were 100% sensitive and 66.7% specific indicators of disease severity. However, in ROC analysis, WBC outperformed CRP in distinguishing between moderate and severe cases, likely due to pronounced leukopenia observed in the severe group. Nevertheless, acute-phase proteins, such as CRP, are approximately eight times more sensitive to inflammatory conditions than WBC counts (Ceron et al. 2005), making CRP a more accurate marker for disease severity.

We observed that CPV-infected dogs had significantly higher levels of pro-inflammatory cytokines and CRP compared to the control group. Similar findings were reported by Ok et al. (2015), who found elevated levels of IL-1ß, TNF-α, INF-γ and CRP in CPV-infected dogs. Increased CRP levels are indicative of inflammation, disease severity and prognosis (Kocaturk et al. 2010; Kocaturk et al. 2015). Elevated IL-6 and TNF-α levels can indicate the severity of inflammation and may aid in diagnosing sepsis (Ok et al. 2015; Song et al. 2012). IFN-γ levels, which are produced in response to viral infections, correlate with the severity of inflammation (Gruys et al. 2006). Our study revealed that although the mild group had higher levels of IL-6 ($p = 0.011$), TNF-α ($p = 0.012$) and IFN-γ, the severe group had notably higher CRP levels. These findings may be interpreted in two ways: First, inflammatory cells release pro-inflammatory cytokines during the acute phase, which triggers the liver to produce acute-phase proteins (Eckersall and Bell 2010; Murata et al. 2004). This could explain the higher cytokine levels in the mild group, consistent with findings by Kocaturk et al. (2015). Second, the observed neutropenia in the severe group may have contributed to the lower cytokine levels, as NEUs and macrophages are key mediators in cytokine release (Ceciliani et al. 2002; Rungelrath et al. 2020). The lower leukocyte levels ($p < 0.05$) in the severe group may thus explain the observed decrease in pro-inflammatory cytokines.

Regarding cardiac biomarkers, both cTnI and CK-MB were elevated in the mild and severe groups compared to controls, with the highest levels observed in the mild group ($p < 0.01$). Notably, cardiac damage can be diagnosed with 100% sensitivity and specificity when cTnI levels exceed 60 ng/L. Cardiac damage, as evidenced by markers such as CK-MB, B-type natriuretic peptide (BNP) (Er and Ok 2015), cTnI (Kocaturk et al. 2012; Gulersoy et al. 2020) and heart-type fatty acid binding protein (H-FABP) (Gulersoy et al. 2020), has been previously reported in CPV-infected dogs. Interestingly, the greater elevation of cardiac markers in the mild group raises an intriguing question. Despite the absence of severe clinical signs, dogs in the mild group exhibited significant cardiac damage, suggesting that myocardial involvement occurs early in the disease. The age distribution of the study groups further supports this observation. The median age of the mild group was 2.25 months (range: 2-3 months), younger than that of the severe group. This finding aligns with the understanding that CPV has a strong tropism for actively proliferating cells, particularly in young animals (Ford et al. 2017). During the neonatal period, cardiomyocytes still exhibit a degree of proliferative capacity, making them more susceptible to viral replication and subsequent damage. This can lead to non-suppurative myocarditis and, in some cases, sudden death from cardiovascular failure (Hayes et al. 1979; Meunier et al. 1984; Lenghaus and Studdert 1984). Moreover, parvoviruses rely on the cellular machinery of mitotically active S-phase cells for viral replication. Therefore, the increased cardiac vulnerability to CPV in neonates may be linked to a higher rate of cardiomyocyte DNA synthesis at this stage, followed by a progressive decline in proliferative activity during postnatal development (Parrish 1995; Parker et al. 2001; Senyo et al. 2013; Bishop 1973). The canine heart has been documented to provide conditions favourable for CPV-2 replication during the neonatal phase up to weaning (Ford et al. 2017). Consequently, given that the dogs in our study averaged 2.5 months of age, we propose that cardiac damage is most pronounced during the early stages of the disease when clinical symptoms are less severe. This observation underscores that sudden death due to cardiac involvement may occur even in mild cases, potentially leading to a poor prognosis. Conversely, in the severe group where clinical symptoms progress, the relatively lower levels of cardiac damage may reflect the immune system's active fight against the virus. Long-term studies have shown that CPV-infected dogs do not experience persistent cardiac problems (Kilian et al. 2018).

CircRNA expression has been associated with the onset and progression of various diseases, including cancer, infections, cardiovascular diseases and neurological disorders (Enuka et al. 2016; Zhong et al. 2018). However, the expression profiles, functions and mechanisms of circRNAs in CPV infection have not been extensively studied.

This study provides the first systematic investigation of circRNA expression in CPV-infected dogs, exploring their potential functions and regulatory mechanisms. Our bioinformatics analysis revealed significant differences in circRNA expression among groups. In the comparison between the mild and control groups, 541 circRNAs were upregulated, whereas 868 were downregulated. In the severe versus control groups, 25 circRNAs were upregulated, whereas 1081 were downregulated. The comparison between the mild and severe groups revealed 753 upregulated and 21 downregulated circRNAs. These findings suggest that these differentially expressed circRNAs play crucial roles in various stages of CPV infection.

Pathway enrichment analysis revealed that a significant proportion of the detected circRNAs regulate cancer-related pathways, including focal adhesion, endocytosis and ErBb signalling. Interestingly, these findings align with prior research on circRNA involvement in viral pathogenesis. For instance, circAcbd6 has been shown to promote cholinergic neuron differentiation via miR-320-5p and Osbpl2 expression (Li et al. 2022), offering a potential mechanistic parallel to CPV infections. Similarly, circRNAs, such as circRNA_000203 and circHIPK3, have been implicated in the inhibition of cardiac fibroblast proliferation and myocardial fibrosis, suggesting a potential protective or pathogenic role, depending on the disease context (Tang et al. 2017; Wu et al. 2021). Furthermore, several of the identified circRNAs participate in Rab1 signalling, ubiquitin-mediated proteolysis and thyroid hormone signalling pathways that play pivotal roles in viral infections. For example, ErbB and Rab1 signallings are known to facilitate viral entry into host cells (Spearman 2018; Ho et al. 2017) with viruses such as influenza A, RSV and coronaviruses utilizing ErbB1 as a key entry mechanism (Ho et al. 2017). Additionally, ubiquitin-mediated proteolysis plays a critical role in viral immune evasion, viral maturation, replication and progeny release (Gao and Luo 2006). These findings suggest that altered circRNA expression in CPV infection may serve as a key regulatory factor in disease pathogenesis, potentially influencing viral replication and host immune responses.

Overlapping circRNAs are a subclass of ncRNAs formed by the back-splicing of exons. Within these overlapping regions, a single circRNA may share sequences with other circRNAs, either from the same gene or from different genes. This structural overlap may impact their regulatory functions, enabling interactions with other circRNAs, sequestration of RNA-binding proteins or competition for miRNA binding sites. Although the functional implications of these overlaps remain under investigation, they are believed to play a complex role in gene regulation and cellular processes (Santer et al. 2019). To further elucidate the roles of these overlapping circRNAs, we conducted an enrichment analysis of the host genes regulated by these circRNAs. GO analysis revealed that the identified circRNAs were primarily involved in biological processes such as cellular protein modification and vesicle-mediated transport, with a focus on molecular functions like kinase activity, iron binding and RNA binding. CPV promotes infection by manipulating host cell protein production and modification processes. For example, the NS1 protein of CPV can suppress host cell protein synthesis, thereby enhancing virus replication (Wang et al. 2024). CPV enters the host cell via endocytosis and is transported through cytoplasmic vesicles to reach the nucleus, where replication and packaging occur (Vihinen-Ranta et al. 2000). The interplay between these processes is critical, as CPV manipulates intracellular and intercellular functions to enhance its pathogenicity. Cellular protein modification increases the virus's ability to invade host cells, whereas vesicle-mediated transport facilitates viral dissemination. The combination of these mechanisms directly contributes to CPV pathogenesis and the clinical course of the disease (Wang et al. 2024; Vihinen-Ranta et al. 2000). CPV infection induces a cascade of physiological changes that facilitate viral replication and contribute to disease progression. Upon infection, CPV preferentially targets rapidly dividing cells, particularly in the intestinal crypts and lymphoid tissues, leading to extensive tissue damage, disruption of gut integrity and immunosuppression. Haematopoietic precursor destruction in the bone marrow results in severe leukopenia, compromising the host's ability to mount an effective immune response. Additionally, CPV infection triggers a robust inflammatory response, characterized by elevated levels of pro-inflammatory cytokines such as IL-6 and TNF-α, which contribute to systemic inflammation and oxidative stress (Aoshi et al. 2011; Harwig et al. 2017). These immune and cellular disruptions collectively drive disease progression, making CPV an ideal model for studying how viral infections alter host cellular pathways. Because viral infections induce a range of physiological changes, including inflammation, oxidative stress, apoptosis and autophagy (Aoshi et al. 2011; Harwig et al. 2017), the progression of CPV infection appears to be strongly associated with these mechanisms. This is further supported by our GO analysis, which identified differentially expressed circRNAs involved in immune responses, cellular transport and inflammatory signalling pathways related to CPV pathogenesis (e.g., cfa_circ_6789, cfa_circ_6793, cfa_circ_6785, and cfa_circ_6798).

Changes in circRNA expression during physiological and pathological conditions have been linked to the progression of various diseases. Physiological conditions, such as growth, development and cellular differentiation, naturally influence circRNA expression patterns, whereas pathological conditions like inflammation, oxidative stress and viral infections, including CPV, lead to significant alterations in circRNA profiles. CPV infection, in particular, induces systemic inflammatory responses, leukopenia and tissue damage, which may contribute to dysregulated circRNA expression (Neyestani et al. 2025). These pathological changes likely affect circRNA biogenesis, stability and function, ultimately influencing immune responses, apoptosis and metabolic regulation (Zhou et al. 2019; Molaei et al. 2023). Our findings support the idea that circRNAs could serve as promising prognostic biomarkers for viral infections (Naeli et al. 2020). In our study, differentially expressed circRNAs were found to be closely associated with key pathological mechanisms of CPV infection. Specifically, we identified circRNAs cfa_circ_3114, cfa_circ_3117, cfa_circ_3118 and cfa_circ_3119 as elevated in the mild group, whereas cfa_circ_6784, cfa_circ_6785, cfa_circ_6786, cfa_circ_6789, cfa_circ_6791, cfa_circ_6793, cfa_circ_6794, cfa_circ_6795 and cfa_circ_6798 were elevated in the severe group. These findings suggest that differential circRNA expression could be used to assess disease severity in CPV infection, with these circRNAs potentially contributing to CPV pathogenesis by regulating inflammatory pathways and immune cell activation. To better categorize their functional significance, we grouped differentially expressed circRNAs based on their associations

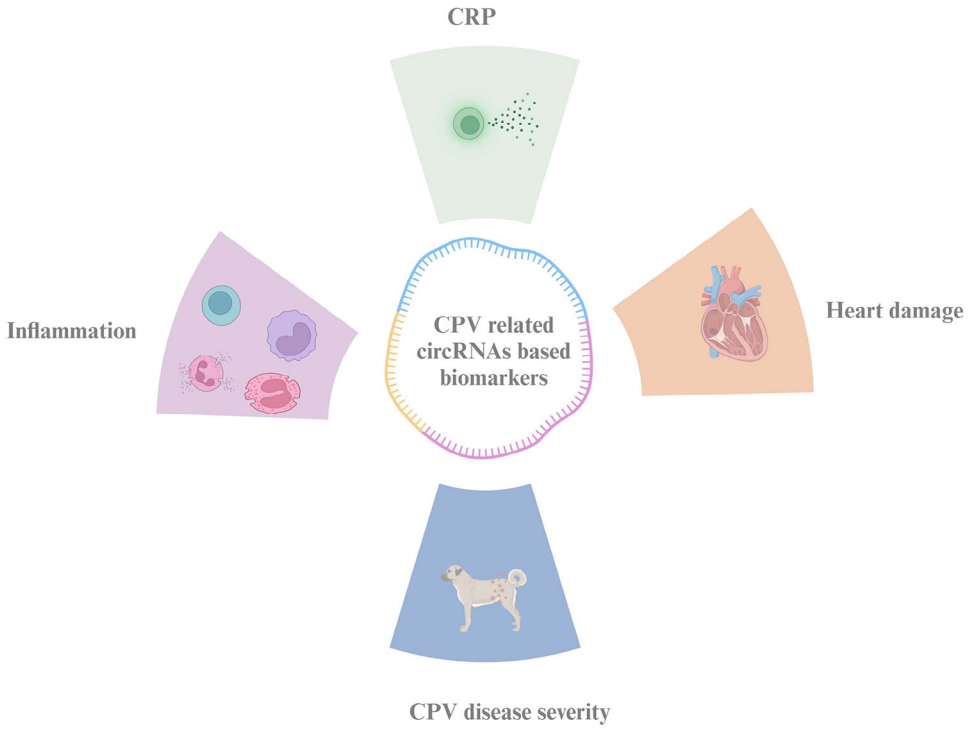

FIGURE 8 | Main outcomes of the study. CPV, canine parvovirus.

with inflammation and cardiac injury. Inflammation-related circRNAs, including cfa_circ_6789, cfa_circ_6793, cfa_circ_6785 and cfa_circ_6798, showed strong positive correlations with CRP levels, suggesting their potential roles in modulating acute-phase responses. Because CRP is a well-established acute-phase protein elevated during systemic inflammation, the upregulation of these circRNAs may indicate their involvement in immune modulation and inflammatory response pathways. On the other hand, cardiac injury-associated circRNAs, such as cfa_circ_3114, cfa_circ_3118, cfa_circ_3117 and cfa_circ_3113, exhibited strong positive correlations with cTnI levels, which are biomarkers of myocardial injury. This finding implicates these circRNAs in CPV-associated myocardial damage, possibly by regulating cardiomyocyte apoptosis or fibrosis. Interestingly, circRNAs, like cfa_circ_1571 and cfa_circ_6786, displayed strong negative correlations with cardiac markers, potentially indicating a compensatory or protective mechanism. Supporting this, Wang et al. (2022) identified two circRNAs in bovine mammary epithelial cells linked to inflammation in bovine mastitis, and circ_0001187 was found to regulate oxidative stress in ulcerative colitis (Ouyang et al. 2022). These findings parallel our study, as CPV-induced inflammation and oxidative stress are major drivers of disease pathology. In both bovine mastitis and ulcerative colitis, circRNAs have been shown to regulate inflammatory cytokine expression, immune cell activation and oxidative damage, mechanisms that are similarly disrupted in CPV infection. This highlights a broader role for circRNAs in viral and inflammatory diseases, reinforcing their potential as molecular targets (Zhang et al. 2021).

CircRNAs have also been implicated in cardiac damage and repair (Zou et al. 2017). For instance, circRNA_000203 is overexpressed in the diabetic myocardium and promotes fibrosis (Tang et al. 2017), whereas circRNA_081881 is downregulated in myocardial infarction, reflecting its role in cardiomyocyte protection (Deng et al. 2016). In CPV infection, myocardial damage is a well-recognized complication, and the observed associations between circRNAs and cardiac markers in our study suggest that circRNAs may influence viral myocarditis by modulating apoptosis and fibrosis pathways. Given these findings, it can be inferred that circRNAs may hold significant promise as diagnostic and prognostic biomarkers in CPV infection. Their strong correlations with established inflammatory (CRP and TNF-α) and cardiac (cTnI and CK-MB) biomarkers suggest they could potentially enhance current diagnostic strategies by providing additional molecular signatures for disease severity and organ involvement. Future studies will be needed to validate these candidate circRNAs and develop qPCR-based assays for early detection and disease monitoring. Furthermore, the potential regulatory functions of circRNAs in CPV pathogenesis warrant further investigation, as targeted modulation of key circRNAs could lead to novel therapeutic approaches.

This study lays the groundwork for understanding the role of circRNAs in virus–host interactions, particularly in the context of CPV infection. Although the sample size was sufficient for initial exploration, further studies with larger cohorts are required to validate the identified circRNAs. Upon confirmation, these circRNAs hold potential as clinical biomarkers for assessing CPV prognosis, organ damage and therapeutic responses (Figure 8). Moreover, understanding their regulatory mechanisms could aid in developing circRNA-based therapeutic interventions, as demonstrated in other diseases such as myocardial fibrosis and inflammatory conditions. Future research could leverage these findings to develop advanced diagnostic tools and treatment approaches for CPV infection.

Author Contributions

Şükrü Değirmençay: Conceptualization, data curation, formal analysis, funding acquisition, investigation, methodology, project administration, resources, supervision, validation, visualization, writing – original draft preparation, writing – review and editing. **Selçuk Özdemir**: Conceptualization, data curation, formal analysis, funding acquisition, investigation, methodology, supervision, writing – original draft, writing – review and editing. **Sefa Küçükler**: Methodology. **Reyhane Bayat**: Writing – review and editing. **Muhammed Kadak**: Writing – review and editing.

Ethics Statement

This study was performed in accordance with the approved ethical rules of Atatürk University (protocol no. 2021/146).

Conflicts of Interest

The authors declare no conflicts of interest.

Data Availability Statement

The data that support the findings of this study are available from the corresponding author upon reasonable request.

The datasets generated during the current study have been deposited in the NCBI database (https://www.ncbi.nlm.nih.gov) under accession number GSE183608. The data can be accessed through this repository.

Peer Review

The peer review history for this article is available at https://www.webofscience.com/api/gateway/wos/peer-review/10.1002/vms3.70344.

References

Aoshi, T., S. Koyama, K. Kobiyama, S. Akira, and K. J Ishii. 2011. "Innate and Adaptive Immune Responses to Viral Infection and Vaccination." *Current Opinion in Virology* 1, no. 4: 226–232. https://linkinghub.elsevier.com/retrieve/pii/S1879625711000538.

Bishop, S. P. 1973. "Effect of Aortic Stenosis on Myocardial Cell Growth, Hyperplasia, and Ultrastructure in Neonatal Dogs." *Recent Advances in Studies on Cardiac Structure and Metabolism* 3: 637–656. http://www.ncbi.nlm.nih.gov/pubmed/4283199.

Brunner, C. 1985. "Canine Parvovirus Infection: Effects on the Immune System and Factors That Predispose to Severe Disease." *Compendium on Continuing Education for the Practicing Veterinarian* 7, no. 12: 979–988.

Ceciliani, F., A. Giordano, and V. Spagnolo. 2002. "The Systemic Reaction During Inflammation: The Acute-Phase Proteins." *Protein & Peptide Letters* 9, no. 3: 211–223. http://www.ncbi.nlm.nih.gov/pubmed/12144517.

Ceron, J. J., P. D. Eckersall, and S. Martýnez-Subiela. 2005. "Acute Phase Proteins in Dogs and Cats: Current Knowledge and Future Perspectives." *Veterinary Clinical Pathology* 34, no. 2: 85–99. http://www.ncbi.nlm.nih.gov/pubmed/15902658.

Chuammitri, P., S. Vannamahaxay, B. Sornpet, K. Pringproa, and P. Patchanee. 2020. "Detection and Characterization of microRNA Expression Profiling and Its Target Genes in Response to Canine Parvovirus in Crandell Reese Feline Kidney Cells." *PeerJ* 8: e8522. http://www.ncbi.nlm.nih.gov/pubmed/32095352.

Conn, S. J., K. A. Pillman, J. Toubia, et al. 2015. "The RNA Binding Protein Quaking Regulates Formation of circRNAs." *Cell* 160, no. 6: 1125–1134. http://www.ncbi.nlm.nih.gov/pubmed/25768908.

Decaro, N., and C. Buonavoglia. 2012. "Canine Parvovirus—A Review of Epidemiological and Diagnostic Aspects, With Emphasis on Type 2c." *Veterinary Microbiology* 155, no. 1: 1–12. http://www.ncbi.nlm.nih.gov/pubmed/21962408.

Deng, Y.-Y., W. Zhang, J. She, et al. 2016. "GW27-e1167 Circular RNA Related to PPARγ Function as ceRNA of microRNA in Human Acute Myocardial Infarction." *Journal of the American College of Cardiology* 68, no. 16: C51–C52. https://linkinghub.elsevier.com/retrieve/pii/S0735109716338773.

Eckersall, P. D. 2004. "The Time Is Right for Acute Phase Protein Assays." *Veterinary Journal* 168, no. 1: 3–5. http://www.ncbi.nlm.nih.gov/pubmed/15158201.

Eckersall, P. D., and R. Bell. 2010. "Acute Phase Proteins: Biomarkers of Infection and Inflammation in Veterinary Medicine." *Veterinary Journal* 185, no. 1: 23–27. http://www.ncbi.nlm.nih.gov/pubmed/20621712.

Enuka, Y., M. Lauriola, M. E. Feldman, A. Sas-Chen, I. Ulitsky, and Y. Yarden. 2016. "Circular RNAs Are Long-Lived and Display Only Minimal Early Alterations in Response to a Growth Factor." *Nucleic Acids Research* 44, no. 3: 1370–1383. http://www.ncbi.nlm.nih.gov/pubmed/26657629.

Er, C., and M. Ok. 2015. "Parvoviral Enteritli Köpeklerde Pıhtılaşma Profilleri Ve Kalp Biyomarkır Düzeyleri." *Kafkas Universitesi Veteriner Fakultesi Dergisi* 21, no. 3: 383–388. http://vetdergi.kafkas.edu.tr/extdocs/2015_3_1/383-388.pdf.

Ford, J., L. McEndaffer, R. Renshaw, A. Molesan, and K. Kelly. 2017. "Parvovirus Infection Is Associated With Myocarditis and Myocardial Fibrosis in Young Dogs." *Veterinary Pathology* 54, no. 6: 964–971. http://www.ncbi.nlm.nih.gov/pubmed/28812526.

Gao, G., and H. Luo. 2006. "The Ubiquitin-Proteasome Pathway in Viral Infections." *Canadian Journal of Physiology and Pharmacology* 84, no. 1: 5–14. http://www.ncbi.nlm.nih.gov/pubmed/16845885.

Goddard, A., and A. L Leisewitz. 2010. "Canine Parvovirus." *The Veterinary Clinics of North America Small Animal Practice* 40, no. 6: 1041–1053. https://linkinghub.elsevier.com/retrieve/pii/S019556161000094X.

Goddard, A., A. L. Leisewitz, M. M. Christopher, N. M. Duncan, and P. J Becker. 2008. "Prognostic Usefulness of Blood Leukocyte Changes in Canine Parvoviral Enteritis." *Journal of Veterinary Internal Medicine* 22, no. 2: 309–316. http://www.ncbi.nlm.nih.gov/pubmed/18371025.

Gruys, E., M. J. M. Toussaint, T. A. Niewold, S. J. Koopmans, E. van Dijk, and R. H Meloen. 2006. "Monitoring Health by Values of Acute Phase Proteins." *Acta Histochemica* 108, no. 3: 229–232. https://linkinghub.elsevier.com/retrieve/pii/S0065128106000365.

Gulersoy, E., M. Ok, R. Yildiz, et al. 2020. "Assessment of Intestinal and Cardiac-Related Biomarkers in Dogs With Parvoviral Enteritis." *Polish Journal of Veterinary Sciences* 23, no. 2: 211–219. http://www.ncbi.nlm.nih.gov/pubmed/32627989.

Harwig, A., R. Landick, and B. Berkhout. 2017. "The Battle of RNA Synthesis: Virus Versus Host." *Viruses* 9, no. 10: 309. http://www.mdpi.com/1999-4915/9/10/309.

Hayes, M. A., R. G. Russell, and L. A Babiuk. 1979. "Sudden Death in Young Dogs With Myocarditis Caused by Parvovirus." *Journal of the American Veterinary Medical Association* 174, no. 11: 1197–1203. http://www.ncbi.nlm.nih.gov/pubmed/438048.

Ho, J., D. L. Moyes, M. Tavassoli, and J. R Naglik. 2017. "The Role of ErbB Receptors in Infection." *Trends in Microbiology* 25, no. 11: 942–952. https://linkinghub.elsevier.com/retrieve/pii/S0966842x17300975.

Kalli, I., L. S. Leontides, M. E. Mylonakis, K. Adamama-Moraitou, T. Rallis, and A. F Koutinas. 2010. "Factors Affecting the Occurrence, Duration of Hospitalization and Final Outcome in Canine Parvovirus Infection." *Research in Veterinary Science* 89, no. 2: 174–178. http://www.ncbi.nlm.nih.gov/pubmed/20303134.

Kilian, E., J. S. Suchodolski, K. Hartmann, R. S. Mueller, G. Wess, and S. Unterer. 2018. "Long-Term Effects of Canine Parvovirus Infection in Dogs." *PLoS One* 13, no. 3: e0192198. https://dx.plos.org/10.1371/journal.pone.0192198.

Kjelgaard-Hansen, M., A. L. Jensen, and A. T Kristensen. 2003. "Evaluation of a Commercially Available Human C-Reactive Protein (CRP) Turbidometric Immunoassay for Determination of Canine Serum CRP

Concentration." *Veterinary Clinical Pathology* 32, no. 2: 81–87. http://www.ncbi.nlm.nih.gov/pubmed/12833223.

Kocaturk, M., S. Martinez, O. Eralp, A. Tvarijonaviciute, J. Ceron, and Z. Yilmaz. 2010. "Prognostic Value of Serum Acute-Phase Proteins in Dogs With Parvoviral Enteritis." *Journal of Small Animal Practice* 51, no. 9: 478–483. http://www.ncbi.nlm.nih.gov/pubmed/20630018.

Kocaturk, M., S. Martinez, O. Eralp, A. Tvarijonaviciute, J. Ceron, and Z. Yilmaz. 2012. "Tei Index (Myocardial Performance Index) and Cardiac Biomarkers in Dogs With Parvoviral Enteritis." *Research in Veterinary Science* 92, no. 1: 24–29. http://www.ncbi.nlm.nih.gov/pubmed/21074228.

Kocaturk, M., A. Tvarijonaviciute, S. Martinez-Subiela, et al. 2015. "Inflammatory and Oxidative Biomarkers of Disease Severity in Dogs With Parvoviral Enteritis." *Journal of Small Animal Practice* 56, no. 2: 119–124. http://www.ncbi.nlm.nih.gov/pubmed/25040669.

Lenghaus, C., and M. J Studdert. 1984. "Acute and Chronic Viral Myocarditis. Acute Diffuse Nonsuppurative Myocarditis and Residual Myocardial Scarring Following Infection With Canine Parvovirus." *American Journal of Pathology* 115, no. 2: 316–319. http://www.ncbi.nlm.nih.gov/pubmed/6326581.

Li, W., B. Shan, X. Cheng, et al. 2022. "circRNA Acbd6 Promotes Neural Stem Cell Differentiation Into Cholinergic Neurons via the miR-320-5p-Osbpl2 Axis." *Journal of Biological Chemistry* 298, no. 4: 101828. https://linkinghub.elsevier.com/retrieve/pii/S002192582200268X.

Livak, K. J., and T. D Schmittgen. 2001. "Analysis of Relative Gene Expression Data Using Real-Time Quantitative PCR and the 2(-Delta Delta C(T)) Method." *Methods (San Diego, California)* 25, no. 4: 402–408. http://www.ncbi.nlm.nih.gov/pubmed/11846609.

Mason, M., N. Gillet, and B. Muggenburg. 1988. "Clinical, Pathological, and Epidemiological Aspects of Canine Parvoviral Enteritis in an Unvaccinated Closed Beagle Colony: 1978–1985." *Journal of the American Animal Hospital Association (USA)* 23, no. 2: 183–192.

Mazzaferro, E. M. 2020. "Update on Canine Parvoviral Enteritis." *The Veterinary Clinics of North America Small Animal Practice* 50, no. 6: 1307–1325. http://www.ncbi.nlm.nih.gov/pubmed/32891439.

Meunier, P. C., B. J. Cooper, M. J. G. Appel, and D. O Slauson. 1984. "Experimental Viral Myocarditis: Parvoviral Infection of Neonatal Pups." *Veterinary Pathology* 21, no. 5: 509–515. https://journals.sagepub.com/doi/10.1177/030098588402100510.

Molaei, P., M. Savari, A. Mahdavinezhad, et al. 2023. "Highlighting Functions of Apoptosis and Circular RNAs in Colorectal Cancer." *Pathology Research and Practise* 248: 154592. https://linkinghub.elsevier.com/retrieve/pii/S0344033823002923.

Mukaka, M. M. 2012. "Statistics Corner: A Guide to Appropriate Use of Correlation Coefficient in Medical Research." *Malawi Medical Journal* 24, no. 3: 69–71. http://www.ncbi.nlm.nih.gov/pubmed/23638278.

Murata, H., N. Shimada, and M. Yoshioka. 2004. "Current Research on Acute Phase Proteins in Veterinary Diagnosis: An Overview." *Veterinary Journal* 168, no. 1: 28–40. http://www.ncbi.nlm.nih.gov/pubmed/15158206.

Mylonakis, M. E., I. Kalli, and T. S Rallis. 2016. "Canine Parvoviral Enteritis: An Update on the Clinical Diagnosis, Treatment, and Prevention." *Veterinary Medicine (Auckland, NZ)* 7: 91–100. http://www.ncbi.nlm.nih.gov/pubmed/30050842.

Naeli, P., M. H. Pourhanifeh, M. R. Karimzadeh, et al. 2020. "Circular RNAs and Gastrointestinal Cancers: Epigenetic Regulators With a Prognostic and Therapeutic Role." *Critical Reviews in Oncology/Hematology* 145: 102854. https://linkinghub.elsevier.com/retrieve/pii/S1040842819302409.

Neyestani, N., K. Madani, D. Shirani, and J. Mehrzad. 2025. "Involvement of Canine Parvovirus in mRNA Expression Levels of Key Lectins and Caspases in Blood Leukocytes." *Veterinary Research Communications* 49, no. 1: 12. https://link.springer.com/10.1007/s11259-024-10586-8.

Ok, M., C. Er, and R. Yıldız. 2015. "Evaluation of Acute Phase Proteins and Cytokines in Dogs With Parvoviral Enteritis." *Eurasian Journal of Veterinary Sciences* 31, no. 3: 143–143. http://eurasianjvetsci.org/pdf/pdf_EJVS_1088.pdf.

Ouyang, W., M. Wu, A. Wu, and H. Xiao. 2022. "Circular RNA_0001187 Participates in the Regulation of Ulcerative Colitis Development via Upregulating Myeloid Differentiation Factor 88." *Bioengineered* 13, no. 5: 12863–12875. https://www.tandfonline.com/doi/full/10.1080/21655979.2022.2077572.

Overholser, B. R, and K. M. Sowinski. 2008. "Biostatistics Primer: Part 2." *Nutrition in Clinical Practice* 23, no. 1: 76–84.

Özdemir, S., N. Aksungur, N. Altundaş, et al. 2022. "Genome-Wide Profiling of the Expression of Serum Derived Exosomal circRNAs in Patients With Hepatic Alveolar Echinococcosis." *Gene* 814: 146161. http://www.ncbi.nlm.nih.gov/pubmed/34995736.

Panda, D., R. C. Patra, S. Nandi, and D. Swarup. 2009. "Oxidative Stress Indices in Gastroenteritis in Dogs With Canine Parvoviral Infection." *Research in Veterinary Science* 86, no. 1: 36–42. https://linkinghub.elsevier.com/retrieve/pii/S0034528808001008.

Parker, J. S. L., W. J. Murphy, D. Wang, S. J. O'Brien, and C. R Parrish. 2001. "Canine and Feline Parvoviruses Can Use Human or Feline Transferrin Receptors to Bind, Enter, and Infect Cells." *Journal of Virology* 75, no. 8: 3896–3902. https://journals.asm.org/doi/10.1128/JVI.75.8.3896-3902.2001.

Parrish, C. R. 1995. "Pathogenesis of *Feline panleukopenia virus* and Canine Parvovirus." *Baillieres Clinical Haematology* 8, no. 1: 57–71. https://linkinghub.elsevier.com/retrieve/pii/S095035360580232X.

Pollock, R. V. 1982. "Experimental Canine Parvovirus Infection in Dogs." *Cornell Veterinarian* 72, no. 2: 103–119. http://www.ncbi.nlm.nih.gov/pubmed/6211333.

Rungelrath, V., S. D. Kobayashi, and F. R DeLeo. 2020. "Neutrophils in Innate Immunity and Systems Biology-Level Approaches." *Wiley Interdisciplinary Reviews: Systems Biology and Medicine* 12, no. 1: e1458. http://www.ncbi.nlm.nih.gov/pubmed/31218817.

Santer, L., C. Bär, and T. Thum. 2019. "Circular RNAs: a Novel Class of Functional RNA Molecules With a Therapeutic Perspective." *Molecular Therapy* 27, no. 8: 1350–1363. http://www.ncbi.nlm.nih.gov/pubmed/31324392.

Segev, G., T. Yaaran, S. Maurice, and G. Baneth. 2022. "Effect of Sampling Site on the Diagnosis of Canine Parvovirus Infection in Dogs Using Polymerase Chain Reaction." *Journal of Veterinary Internal Medicine* 36, no. 2: 591–598. http://www.ncbi.nlm.nih.gov/pubmed/35090069.

Şentürk, H., and E. Kömürcü Bayrak. 2019. "Kardiyovasküler Hastalıklarda Uzun Kodlamayan RNA'lar Ve Sirküler RNA'ların Önemi." *Istanbul University Institute of Health Sciences Journal of Advanced Research in Health Sciences* 2, no. 3: 115–125. http://iupress.istanbul.edu.tr/journal/jarhs/article/kardiyovaskuler-hastaliklarda-uzun-kodlamayan-rnalar-ve-sirkuler-rnalarin-onemi.

Senyo, S. E., M. L. Steinhauser, C. L. Pizzimenti, et al. 2013. "Mammalian Heart Renewal by Pre-Existing Cardiomyocytes." *Nature* 493, no. 7432: 433–436. https://www.nature.com/articles/nature11682.

Song, R., J. Kim, D. Yu, C. Park, and J. Park. 2012. "Kinetics of IL-6 and TNF-α Changes in a Canine Model of Sepsis Induced by Endotoxin." *Veterinary Immunology and Immunopathology* 146, no. 2: 143–149. http://www.ncbi.nlm.nih.gov/pubmed/22424937.

Spearman, P. 2018. "Viral Interactions With Host Cell Rab GTPases." *Small GTPases* 9, no. 1–2: 192–201. http://www.ncbi.nlm.nih.gov/pubmed/28696820.

Swets, J. A. 1988. "Measuring the Accuracy of Diagnostic Systems." *Science* 240, no. 4857: 1285–1293. https://www.science.org/doi/10.1126/science.3287615.

Tang, C.-M., M. Zhang, L. Huang, et al. 2017. "CircRNA_000203 Enhances the Expression of Fibrosis-Associated Genes by Derepressing Targets of

miR-26b-5p, Col1a2 and CTGF, in Cardiac Fibroblasts." *Scientific Reports* 7, no. 1: 40342. https://www.nature.com/articles/srep40342.

Vihinen-Ranta, M., W. Yuan, and C. R Parrish. 2000. "Cytoplasmic Trafficking of the Canine Parvovirus Capsid and Its Role in Infection and Nuclear Transport." *Journal of Virology* 74, no. 10: 4853–4859. https://journals.asm.org/doi/10.1128/jvi.74.10.4853-4859.2000.

Wang, J.-P., J. Yang, P. Jiao, et al. 2022. "Differential Expression of circRNAs Related to Lipopolysaccharide-Induced Inflammation in Bovine Mammary Epithelial Cells." *Research in Veterinary Science* 146: 24–27. https://linkinghub.elsevier.com/retrieve/pii/S003452882200073X.

Wang, X., X. Hao, Y. Zhao, X. Xiao, S. Li, and P. Zhou. 2024. "Canine Parvovirus NS1 Induces Host Translation Shutoff by Reducing mTOR Phosphorylation." *Journal of Virology* 99: e0146324. https://journals.asm.org/doi/10.1128/jvi.01463-24.

Wu, N., C. Li, B. Xu, et al. 2021. "Circular RNA mmu_circ_0005019 Inhibits Fibrosis of Cardiac Fibroblasts and Reverses Electrical Remodeling of Cardiomyocytes." *BMC Cardiovascular Disorders [Electronic Resource]* 21, no. 1: 308. https://bmccardiovascdisord.biomedcentral.com/articles/10.1186/s12872-021-02128-w.

Zhong, Y., Y. Du, X. Yang, et al. 2018. "Circular RNAs Function as ceRNAs to Regulate and Control Human Cancer Progression." *Molecular cancer* 17, no. 1: 79. http://www.ncbi.nlm.nih.gov/pubmed/29626935.

Zhou, P., X. Zhang, W. Zeng, et al. 2017. "MicroRNA Expression Analysis of Feline and Canine Parvovirus Infection In Vivo (*Felis*)." *PLoS ONE* 12, no. 10: e0185698. http://www.ncbi.nlm.nih.gov/pubmed/29049413.

Zou, M., C. Huang, X. Li, et al. 2017. "Circular RNA Expression Profile and Potential Function of hsa_circRNA_101238 in Human Thoracic Aortic Dissection." *Oncotarget* 8, no. 47: 81825–81837. https://www.oncotarget.com/lookup/doi/10.18632/oncotarget.18998.

Zhou, Z., B. Sun, S. Huang, and L. Zhao. 2019. "Roles of Circular RNAs in Immune Regulation and Autoimmune Diseases." *Cell Death and Disease* 10, no. 7: 503. https://www.nature.com/articles/s41419-019-1744-5.

Zhang, Y., Y. Chen, Y. Wan, et al. 2021. "Circular RNAs in the Regulation of Oxidative Stress." *Frontiers in Pharmacology* 12. https://www.frontiersin.org/articles/10.3389/fphar.2021.697903/full.

Supporting Information

Additional supporting information can be found online in the Supporting Information section.